

34 MHz $\lambda/4$ Spiral Resonator

Hiroshi FUJISAWA*, Takao MATSUMOTO* and Masayuki TAMADA*

Received February 9, 1994

A 34 MHz $\lambda/4$ spiral resonator has been constructed and installed as a post accelerator/decelerator of the existing 4-rod RFQ¹⁾. The resonator is made of aluminum and has two accelerating gaps. A measured unloaded Q-value Q_0 and shunt impedance R_0 are 1670 and 741 k Ω , respectively. The total acceleration voltage of 86 kV is expected at the rf power of 5 kW. The resonator has been rf-power tested up to 5 kW cw and the preliminary beam acceleration tests have been done using He⁺ and N²⁺ ion beams.

KEY WORDS: Spiral resonator / Post-accelerator / rf cavity / $\lambda/4$ resonator

1. MOTIVATION

Energy variability is essential in the applications of ion implantation. Since beam energy is invariable in a fixed-frequency RFQ, we need to introduce a means to realize that requirement. We have proposed an addition of a spiral $\lambda/4$ resonator as a post-accel./decel. structure to our RFQ²⁾. This type of resonator is especially suitable in low rf frequency since a normal straight-stem $\lambda/4$ resonator becomes too large in practice. If an energy range is not too wide, we may achieve the goal by just adding one resonator. If we require wide energy variability, then such a resonator could be used in series.

2. SPIRAL RESONATOR

Design

The design of this resonator is based on the 1/3 model studies done back in 1990²⁾. The construction of the resonator reflects the results of those model studies except for a change in material; from copper to aluminum. This decision is made because higher costs and copper contamination are to be avoided in most of industrial applications.

Fig. 1 depicts the definitions of dimensions of the spiral resonator; the specification of the resonator are given in table 1. Photo. 1 is a picture of the spiral resonator being assembled by one of the authors. In the cavity, there are eight vacuum ports that are allocated for various uses: a drive loop, a frequency tuner, a port to turbo-molecular pump, a spiral's stem fixture, and a view window. The cavity, the drive loop, the frequency tuner, and the spiral are all water cooled. A 400 l/s turbo-molecular pump is installed exclusively for the resonator. A typical vacuum level without rf is about 1.0×10^{-6} Torr.

*藤沢 博、松本貴男、玉田将之 : Nissin Electric Co., Ltd.

34 MHz $\lambda/4$ Spiral Resonator

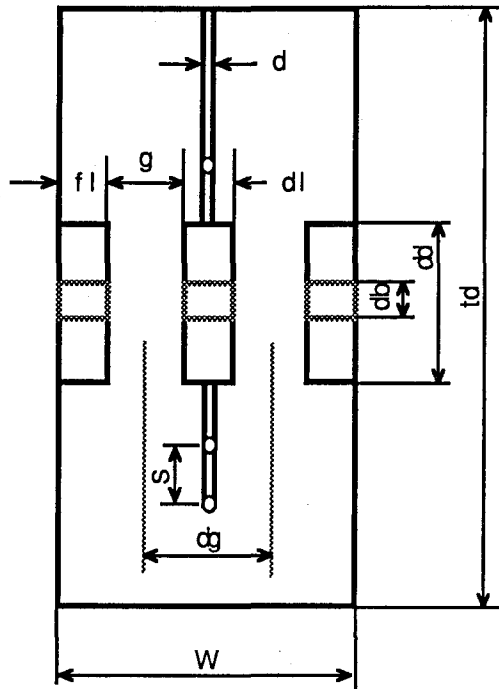


Fig. 1 Definitions of dimensions of 34 MHz spiral resonator.

Table 1. Specification of spiral resonator.

Gap length, g	21.0 mm
Diameter of drift tube, dd	96.0 mm
Bore diameter, db	24.0 mm
Gap-gap length, dg	60.0 mm
Length of drift tube, dl	39.0 mm
Length of field cut-off tube, fl	19.5 mm
Separation pitch, s	54 mm
Diameter of tube, d	21 mm
Width of resonator, w	120 mm
Diameter of tank, td	600 mm
Resonant frequency (MHz)	33.9 MHz
Unloaded Q value, Q_0	1670
Shunt impedance/resonator, R_0	741 k Ω

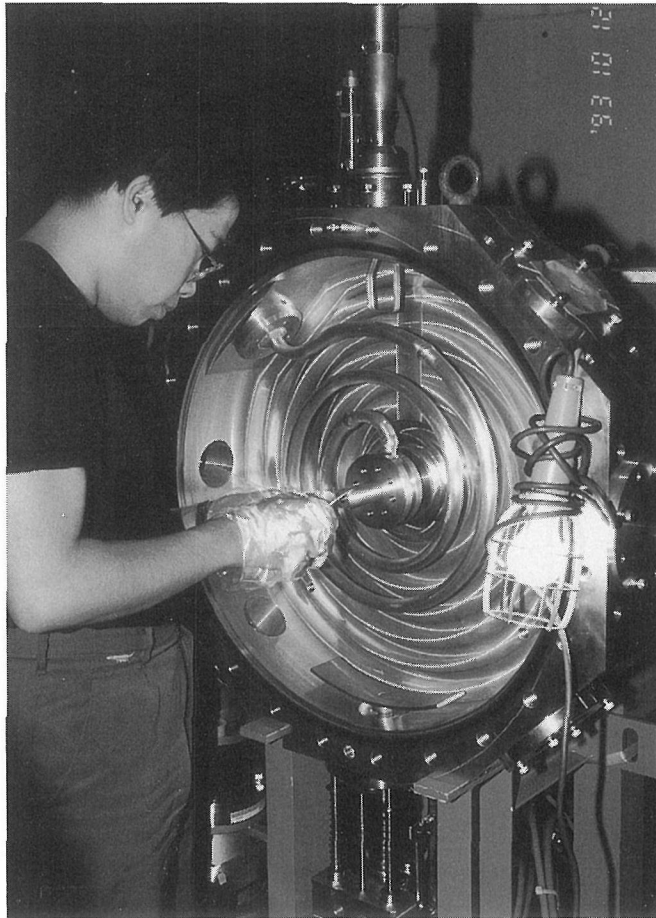


Photo. 1 Picture of 34 MHz spiral resonator.

Cold test

The characteristic impedance R_o/Q_o of the resonator was measured by a bead-pull method. The bead is a metal-plated plastic ball, 10 mm in diameter. Fig. 2 represents a typical results of the measurements. The value R_o/Q_o is estimated to be 452Ω per resonator. The measured unloaded Q -value Q_o is 1640 so that the shunt impedance R_o is approximately $741\text{ k}\Omega$ per resonator. The frequency tuner installed at the bottom of the resonator is capable to tune the resonant frequency in a span of 80 kHz.

High power test

A high power test has been performed up to 5 kW, which is the maximum output power of the rf amplifier³⁾. The trends in the initial power tests can be seen in fig. 3, where the resonant frequencies of the resonator are plotted against the value of rf power. One can see a relatively large frequency shift of approximately 10 kHz/kW. The vibrations from the running water or from any other possible sources may cause the instability in this type of resonator.

34 MHz $\lambda/4$ Spiral Resonator

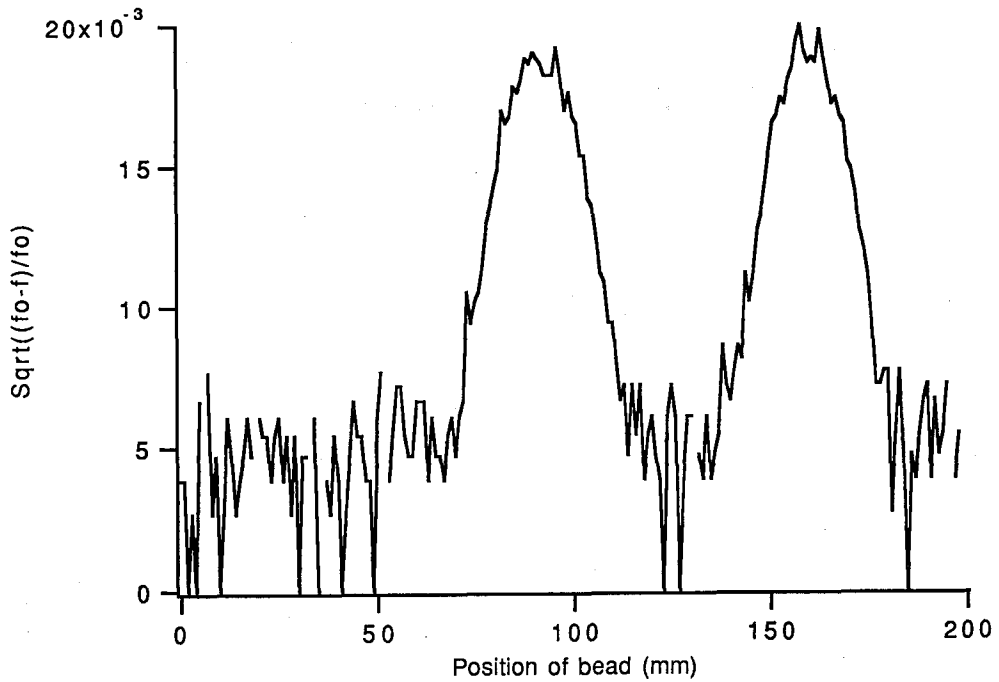


Fig. 2 A typical bead-pull data for 34 MHz spiral resonator.

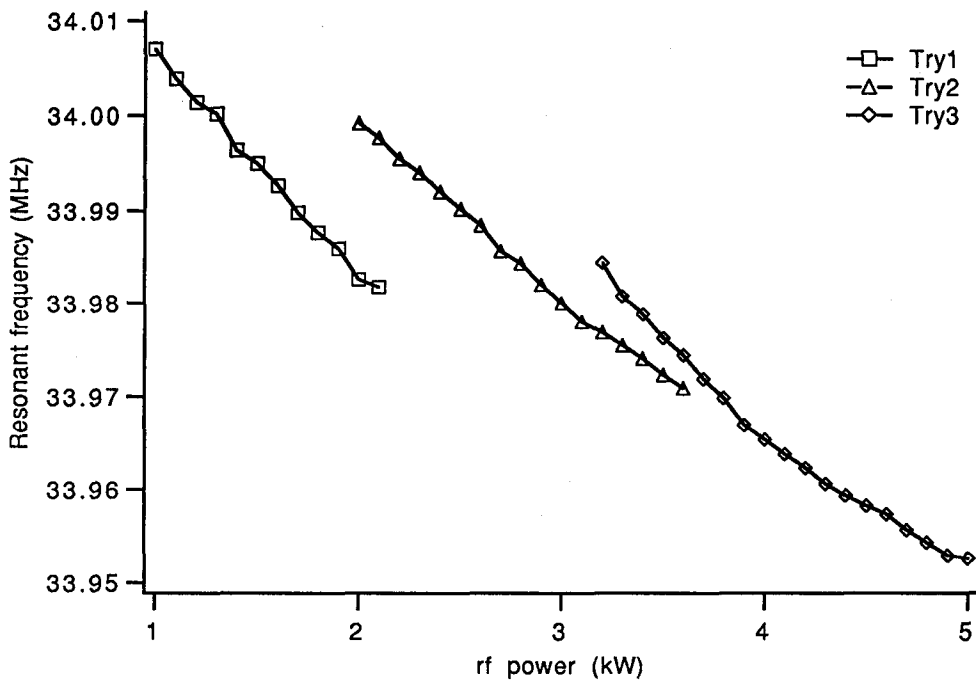


Fig. 3 Frequency shift as a function of rf power in the initial rf power test for 34 MHz spiral resonator.

Our resonator has shown no sign of such a problem, however.

3. BEAM TESTS AND ANALYSIS

Photo. 2 shows an experiment setup of the beam tests. From the right to left shown in the picture are a 4-rod RFQ cavity, a spiral resonator, a 15° degree magnet, and a Faraday cup

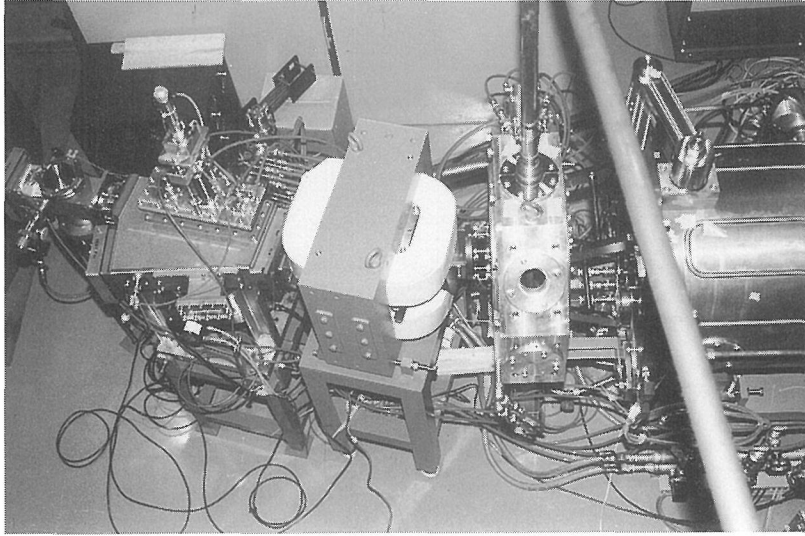


Photo. 2 Experiment setup of spiral resonator beam tests.

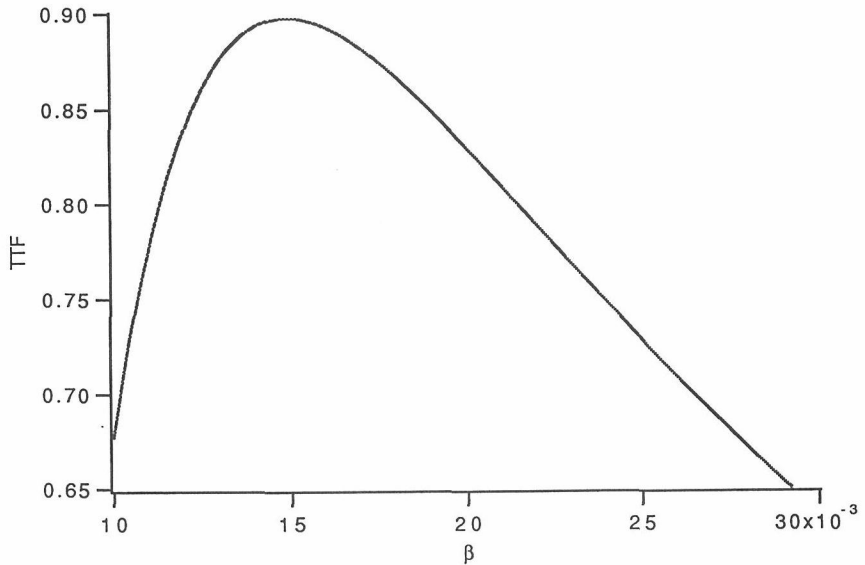


Fig. 4 Transit time factor (TTF) as a function of β for 34 MHz spiral resonator.

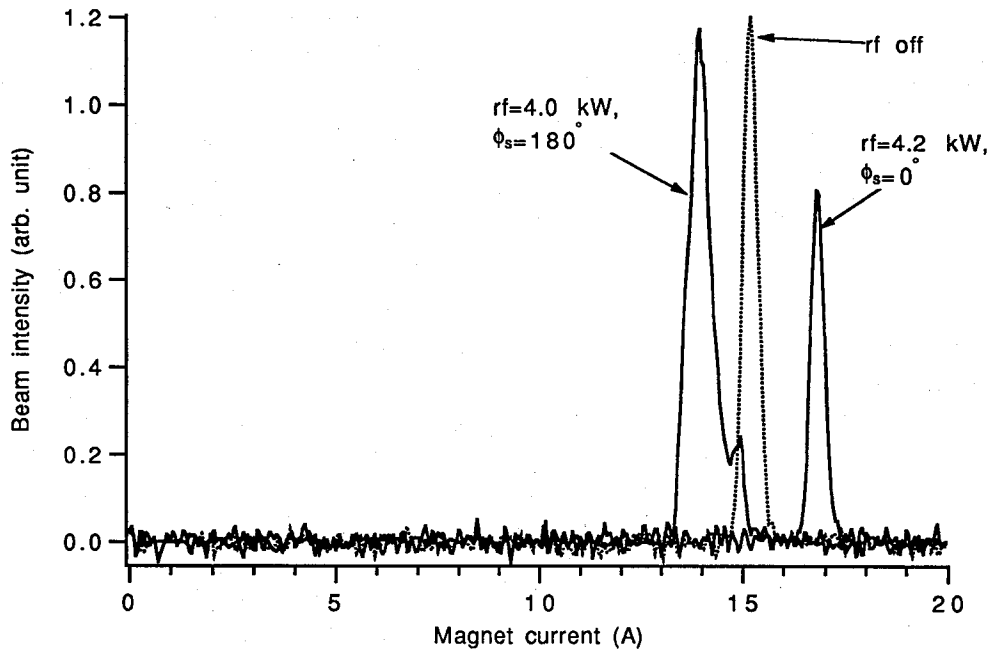


Fig. 5 Momentum spectra of a He^+ beam.

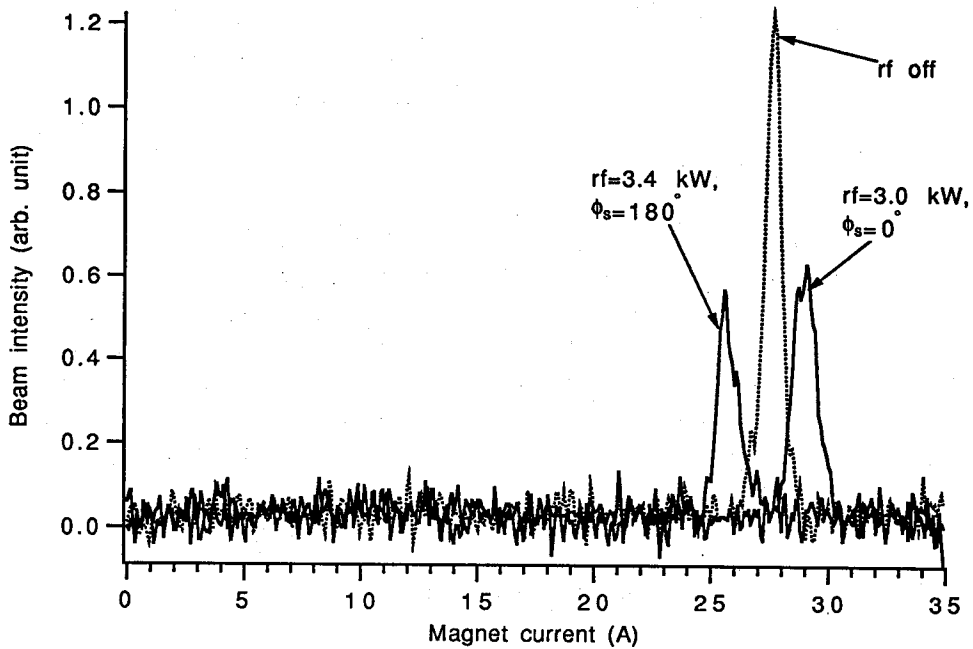


Fig. 6 Momentum spectra of a N^{2+} beam.

Table 2. Summary of beam acceleration tests.

	rf power (kW)	Mag. current (A)	ΔE (KeV)
He ⁺ : power off	0	15.2	0
$\phi_s = 0^\circ$	4.2	16.8	+73
$\phi_s = 180^\circ$	4.0	13.9	-59
N ²⁺ : power off	0	27.6	0
$\phi_s = 0^\circ$	3.0	29.0	+109
$\phi_s = 180^\circ$	3.4	25.7	-148

system. A beam emerges out of the RFQ and enters the spiral resonator. The beam is then momentum analyzed with the 15° degree magnet and Faraday cup system. The beam is collimated both at the entrance and exit of the magnet to get the mass resolution ($M/\Delta M$) 50.

Fig. 4 shows calculated transit time factor (TTF) as a function of particle velocity β ^{4,5,6}. The synchronous β of a particle coming out of the RFQ is 0.0136 so that TTF is about 0.89 from the figure. Also recognizable from fig. 4 is a wide range of energy acceptability. Suppose that the minimum value of TTF is set to be 0.8, then the acceptable range of β extends from 0.0113 to 0.0214. This corresponds to an energy range of 60 keV/u. to 213 keV/u. Fig. 5 and 6 are the results of the beam tests for He⁺ and N²⁺, respectively. In both figures, the middle peak represents a "through beam", meaning no rf power is fed to the spiral resonator. In this case the energy of a beam is the synchronous energy of the RFQ output: 346 keV and 1071 keV for He⁺ and N²⁺, respectively. The peak right to the middle one represents an accelerated beam (phase is set to 0°) and the left one a decelerated beam (phase is set to 180°). An analysis of energy gains based on the synchronous energies and the magnet currents is summarized in table 2.

An energy gain ΔE in the spiral resonator is found as follows⁷:

$$\Delta E = q V_t TTF \cos \phi_s, \quad (1)$$

where q = charge state, V_t = total acceleration voltage,
 TTF = transit time factor, and ϕ_s = synchronous phase.

Fig. 7 and 8 are the absolute value of ΔE plotted as a function of rf power fed into the spiral resonator for $q = 1$ and $q = 2$, respectively. In the calculations, an experimentally obtained value of the shunt impedance $R_o = 741 \text{ k}\Omega$ is used. Data obtained in the beam tests are imposed in those figures for comparison. In both He⁺ and N²⁺ cases, the agreements are satisfactory.

4. CONCLUDING REMARKS

It has been proved that a spiral resonator is suitable for low frequency post accel./decel. structure to an RFQ. The energy gain obtained in the beam tests shows a quite good agree-

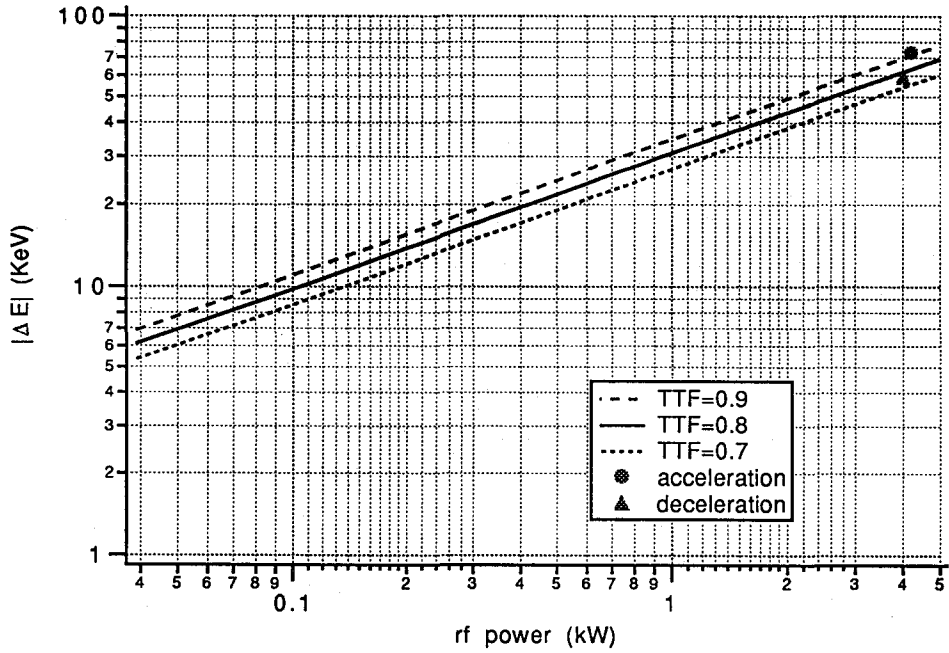


Fig.7 Plots of $|\Delta E|$ as a function of rf power for singly-charged ion beam. Experimentally obtained data for He^+ beam are indicated as dots.

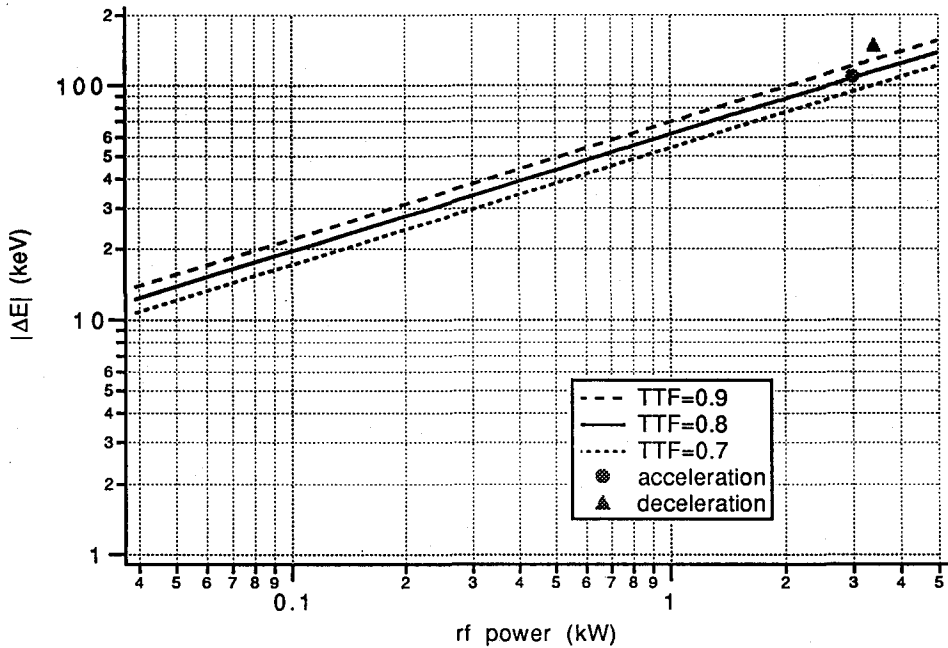


Fig.8 Plots of $|\Delta E|$ as a function of rf power for doubly-charged ion beam. Experimentally obtained data for N^{2+} beam are indicated as dots.

ment with the theory. Metal contamination and total beam current are the subjects of study planned in the next step.

5. ACKNOWLEDGEMENT

The authors would like thank Prof. Makoto Inoue and Prof. Akira Noda, and Yoshihisa Iwashita of Institute for Chemical Research, Kyoto University for continuing support to proceed with this project at their facility. Their advises and encouragement are invaluable for the success of this project.

REFERENCES

- (1) H. Fujisawa, et al., "Beam Tests of a cw 4-rod RFQ", Proceedings of the 9th Symposium on Accelerator Science and Technology (1993) pp.146-148.
- (2) H. Fujisawa, et al., "Design Study of a Heavy Ion RF Linac for MeV Implanter", Proceedings of the 1990 LINAC Conf., LA-12004-C (1990) pp.241-243.
- (3) H. Fujisawa, "The RF Power Amplifier System for a Heavy Ion RFQ Linac", *Bull. Inst. Chem. Res. Kyoto Univ.*, Vol.69, No.1, (1991) pp.11-14.
- (4) A. Schempp and H. Klein, "Properties of Spiral Loaded Cavities", *Nucl. Instrum. Methods*, **135**, (1976) pp.409-414.
- (5) A. Schempp, et al., "Measurements on Spiral Resonators at High Field Level", *Nucl. Instrum. Methods*, **140**, (1977) pp.1-7.
- (6) I. Ben-Zvi and J.M. Brennan, "The Quarter Wave Resonator as a Superconducting Linac Element", *Nucl. Instrum. Methods*, **212**, (1983) pp.73-79.
- (7) E. Jaeschke et al., "The Heidelberg 3MV-CW Heavy Ion Postaccelerator Section Using Independent Phased Spiral Resonators", *IEEE Trans. on Nuclear Science*, Vol.NS-24, No.3 (1977) pp.1136-1139.